Failure analysis of three rigid block assemblies – A real collapse resulting in death

Giada Frappa *, Margherita Pauletta, Gaetano Russo

Polytechnic Department of Engineering and Architecture, University of Udine, Via delle Scienze 206 – 33100 Udine, Italy

ARTICLE INFO

Keywords:
Rigid block assembly
Artefact
Experimental tests
Overturning stability
Maintenance error
Stabilization of connections

ABSTRACT

The failure analysis of three rigid block assemblies is often necessary to assess the stability of architectural and historical assets.

An analytical method for the assessment of the overturning stability of assemblies composed by three rigid blocks fitted atop one on another is proposed. The method takes account of several load configurations and all possible collapse mechanisms involving the overturning of one, two or three blocks.

In the category of historical assets fall many holy water stoups with pillar, often realized as three rigid block assemblies. A great number of holy water stoups disarticulations occurred in Italy in the last decades, leading, in some cases, to children death.

A 7 years old girl died due to the disarticulation of an historical holy water stoup in the Santa Chiara Church, in Udine, Italy, caused by the force applied by the girl on the basin.

The stoup is realized as a three rigid block assembly with connections of the type mortise and tenon both between the basement and the shaft and between the shaft and the basin. In the connections the presence of mortar is detected. In order to evaluate the ability of the mortar to stabilize the connections between the three rigid blocks, the mineralogical and petrographic analyses of a mortar sample are performed. Moreover, a loading test is carried out in laboratory to obtain an experimental value of the holy water stoup failure load. This value is determined by applying a vertical force to the outer circumference of the basin.

Then, in order to determine the holy water stoup failure load under an inclined force statically applied at the top of the basin, the stoup overturning stability is theoretically analysed. The analysis is performed considering all possible collapse mechanisms of the three rigid block assembly and the variability of the force inclination with respect to the horizontal plane. The performed analysis is suitable because it confirms that the disarticulation of the holy water stoup can be caused by a force applied by the kid at the top of the basin.

The presented paper is the first one that analyses the overturning stability of three rigid block assemblies under external forces which do not depend on the single blocks masses and with variable direction.

1. Introduction

On 21st November 2019, a 7 years old girl died due to the overturning of an historical holy water stoup, which dated back to 1646.

* Corresponding author.
E-mail addresses: giada.frappa@uniud.it (G. Frappa), margherita.pauletta@uniud.it (M. Pauletta), gaetano.russo@uniud.it (G. Russo).

The event occurred in the Santa Chiara Church, in Udine, as referred in [1–3]. The failure of the holy water stoup was due to its disarticulation in the three rigid blocks composing it, under the forces exerted by the girl on the basin. Such an accident and the consequent manslaughter proceeding occurred in the case study considered herein. In addition to this event, other seven cases of disarticulation of ancient holy water stoups, realized as three rigid block assemblies, occurred in Italy from 1971 to 2018. These cases are the following:

- Church of Santissimo Crocifisso, in Bravetta (in the province of Rome) – 1971 [4];
- Church of San Giovanni Battista, in Siniscola (in the province of Nuoro) – 1996 [5];
- Church of Gesù Redentore, in Serre (in the province of Salerno) – 2001 [6];
- Church of the Rosary, in Santo Stefano di Camastra (in the province of Messina) – 2003 [7];
- Church of the Rosary, in Mareno di Piave (in the province of Treviso) – 2014 [8];
- Church of Santi Ippolito e Cassiano, in Alfianello (in the province of Brescia) – 2015 [9];
- Church of Solarolo, in Goito (in the province of Mantova) – 2018 [10].

In all the cases mentioned above, the collapse of the holy water stoups was caused by forces exerted by children, even of early age. The falling of blocks induced serious injuries to the children and, sometimes, even the death.

Holy water stoups with pillar are artefacts realized as three rigid block assemblies.

The great number of accidents due to holy water stoups disarticulation highlights that this risk is high and, thus, it cannot be neglected in the safety assessment of places that host them. It also points out the high vulnerability of historical artistic assets realized as rigid block assemblies, which in Italy constitute a not negligible part of the cultural heritage. It follows that, in order to guarantee that visitors could enjoy this cultural heritage in safe conditions, it is fundamental to assess its safety respect to all possible collapse mechanisms that it could be subjected to and which are dangerous for human life. In particular, with regard to holy water stoups, their overturning stability has to be assessed. For these type of historical assets the static friction coefficient between two consecutive blocks as well as the lower block and the ground is large enough to hinder sliding between two consecutive blocks and between the lower block and the ground, as made by Kounadis et al. in [11]. The overturning stability analysis is the basis for a subsequent intervention aimed to provide them with adequate stability.

In the literature, overturning stability of structures made by three rigid block assemblies is dealt in very few research works [11–12] and it is always analyzed under horizontal dynamic actions, simulating earthquake excitations. Among these works, in [11] the overturning stability is studied assuming that friction forces, between consecutive blocks and between the lower block and the ground, are large enough to prevent sliding mechanisms. Instead, in [12] the overturning stability is studied considering coupling with sliding. Nevertheless, in light of the above, the collapse of three rigid block assemblies may be caused also by load conditions different from those involved by ground motions, as occurs for many architectural and historical assets. In particular, the failure of these assets can be caused by forces exerted by people, even of little magnitude, as those exerted by kids. Consequently, the overturning stability should be evaluated considering all possible actions that can be exerted by people. The analysis should take account that the actions mentioned above may be applied in any point or area of the three rigid block assembly and that their direction is unknown.

The aim of this research is to propose a method to perform the overturning stability analysis of three rigid block assemblies often constituting the structure of historical assets, under static load conditions (Fig. 1). The presented paper is the first one that analyses the overturning stability of three rigid block assemblies under external forces which do not depend on the single blocks masses and with variable direction.

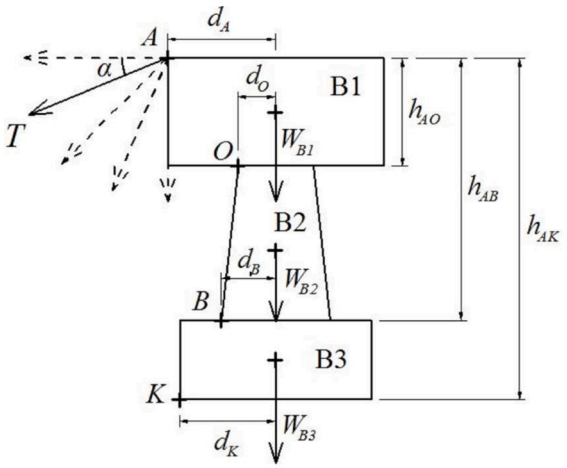

Fig. 1. A three rigid block assembly under the force T applied at one of the top corners.

2. Method for the overturning stability analysis

The analytical assessment of the overturning stability of assemblies composed by three rigid blocks fitted atop one on another consists in the formulation of the rotational equilibrium equations of the assembly, under external forces and under different hypotheses of disarticulation mode, as made in [12]. The proposed method takes account of several load configurations and all possible collapse mechanisms of the three rigid block assembly under a force T statically applied at one of the top corners of the upper block (Fig. 1). In particular, with respect to the assembly represented in Fig. 1, the possible collapse mechanisms are:

1) the overturning of only the upper block B1 around point O,

2) the rigid body overturning of the assembly composed by the upper and the middle block, B1 and B2 respectively in Fig. 1, around point B, and.

3) the overturning of the whole assembly composed by blocks B1, B2 and B3, as a rigid body, around point K.

The failure analysis must take into account all the three mentioned mechanisms. The arising mechanism depends on the dimensions and the weight of the three blocks as well as the construction details of the connections between them. Thus, the method application to a specific case requires that the above mentioned parameters relative to the case are taken into account. In particular, in order to properly model the kinematic behavior of rigid block assemblies, an accurate geometrical and dimensional survey of connections is fundamental. The assessment of connections rigidity allows to properly evaluate their ability to warrant the blocks rotation around point O, or B, or K.

In the overturning stability analysis of the assembly under the inclined force T it is assumed that the centroid axes of the three elements of the assembly are aligned with each other.

It is assumed that no linking elements are present in the connections and that rotations and upward vertical displacements of the upper block relative to the middle block and of the latter relative to the lower block are allowed.

Since the inclined force T is applied to the upper block, B1 in Fig. 1, it has to be checked, for each considered value of the inclination angle, α, of T from the horizontal plane, if it involves the overturning mechanism of one, two or three blocks.

2.1. Mechanism 1: One block overturning

One block overturning collapse mechanism consists in the upper block rotation around point O (Fig. 1), which belongs to the boundary of the contact surface between the upper and the middle blocks.

The forces involved in the rotational equilibrium of the upper block are T and the self-weight W_{B1}, as shown in Fig. 1. The rotational equilibrium equation of the upper block around point O is expressed as follows.

$$W_{B1} \bullet d_O = T cos\alpha \bullet h_{AO} + T sen\alpha \bullet (d_A - d_O) \tag{1}$$

where d_O is the distance between point O and the upper block vertical axis, h_{AO} is the lever arm of the horizontal component of force T with respect to point O and d_A is the distance between the force application point and the assembly vertical axis.

2.2. Mechanism 2: Two blocks assembly overturning

The rotation of the upper and middle block assembly as a rigid body occurs around a point B belonging to the boundary of the contact surface between the middle and the lower blocks (Fig. 1).

The rotational equilibrium of the upper-middle blocks assembly is governed by the applied force T and the self-weights of the upper and middle blocks, W_{B1} and W_{B2}, respectively (Fig. 1). The rotational equilibrium of the assembly with respect to point B (Fig. 1) provides the following equation.

$$(W_{B1} + W_{B2}) \bullet d_B = T cos\alpha \bullet h_{AB} + T sen\alpha \bullet (d_A - d_B) \tag{2}$$

where d_B is the distance between point B and the assembly vertical axis and h_{AB} is the lever arm of the horizontal component of force T with respect to point B.

2.3. Mechanism 3: Whole assembly overturning

The rotation of the upper, middle and lower blocks assembly as a rigid body occurs around a point K belonging to the boundary of the contact surface between the lower block and the floor (Fig. 1).

The rotational equilibrium of the three blocks assembly is governed by the applied force T and the self weights of the upper, middle and lower blocks, W_{B1}, W_{B2} and W_{B3}, respectively (Fig. 1). The rotational equilibrium of the assembly with respect to point K provides the following equation.

$$(W_{B1} + W_{B2} + W_{B3}) \bullet d_K = T cos\alpha \bullet h_{AK} + T sen\alpha \bullet (d_A - d_K) \tag{3}$$

where d_K is the distance between point K and the assembly vertical axis and h_{AK} is the lever arm of the horizontal component of force T with respect to point K.

3. Case study

In this study the overturning stability of the holy water stoup of Santa Chiara Church, under a statically applied force, is analysed as case-study. This holy water stoup is composed by three marble elements named as basement, shaft and basin, as shown in Fig. 2(a). The connections between the basement, A in Fig. 3, and the shaft, B in Fig. 3, and between the shaft and the basin, C in Fig. 3, are of the type mortise and tenon. The surfaces of the mortises and the tenons are covered by mortar.

The weight measurement and the geometrical and dimensional survey of the three elements was carried out by the Mechanics of Materials Laboratory of the University IUAV of Venice. The weights of the basement, the shaft and the basin are equal to 1313.1 N, 513.9 N and 2335 N, respectively. The main dimensions of the holy water stoup elements are shown in Fig. 2. In this figure and in the following description the dimensions of the tenons and the mortises include the covering mortar layer.

During the accident, caused by the disarticulation of the holy water stoup, the three elements got separated from each other, as shown in the photo in Fig. 3, taken after the accident.

3.1. Basement-shaft connection

In the lower connection between the basement and the shaft, the mortise is at the top of the basement and the tenon is at the bottom of the shaft.

The mortise (in Fig. 2(b)) is defined by a cylindrical hollow, of diameter 152 mm and depth 33.4 mm, having a stone prominence with circular segment plan-form, indicated with a red arrow in Fig. 4. The prominence protrudes from the bottom plane surface of the hollow and leans against its vertical surface. The length of the straight side of the stone prominence, measured on the bottom plane surface of the hollow, is equal to 68 mm.

The prominence of the mortise imposes the presence, in the shaft bottom tenon, of a cylindrical-conical indentation having a complementary shape to that of the prominence.

The mean values of the tenon diameter and height are equal to 148 mm and 35.9 mm, respectively. The length of the straight side of the tenon indentation, measured on the bottom plane surface of the tenon, is equal to 86 mm.

From the comparison between the mortise and tenon diameters (Fig. 5), it is deduced that between the tenon and the mortise there

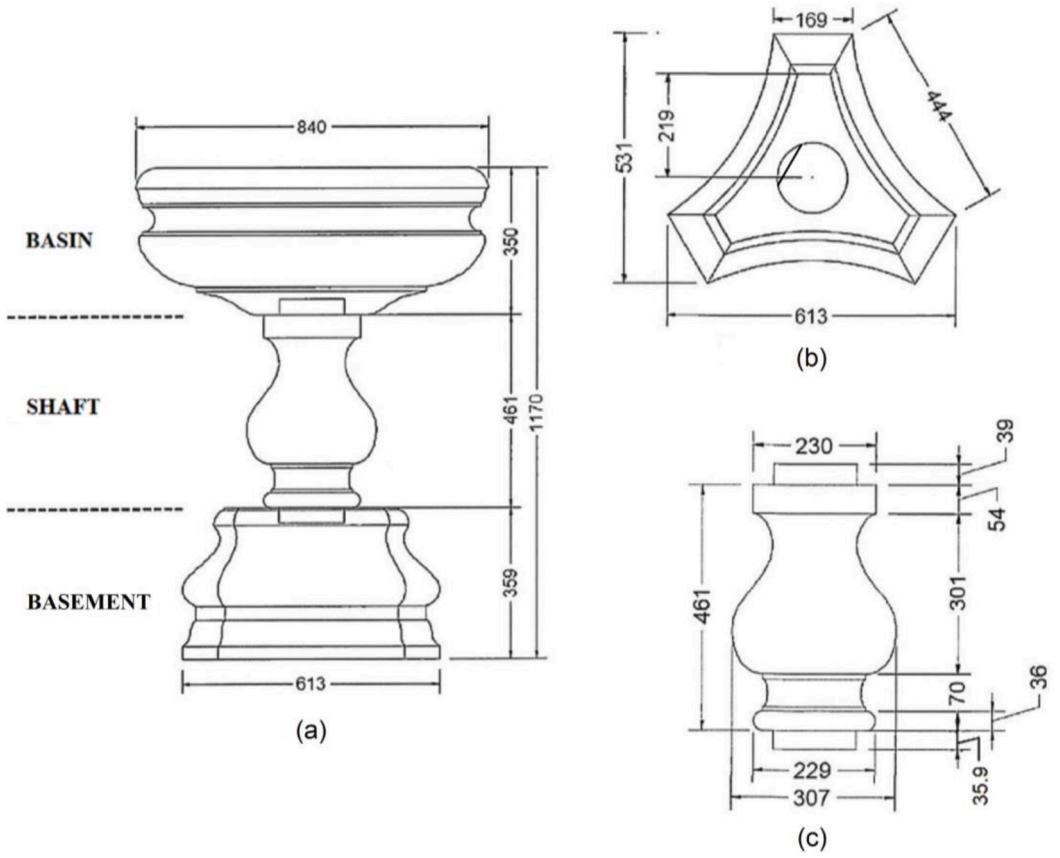

Fig. 2. Geometric and dimensional characteristics of the holy water stoup: assembly front view (a), basement plan view (b) and shaft front view (c), dimensions in mm.

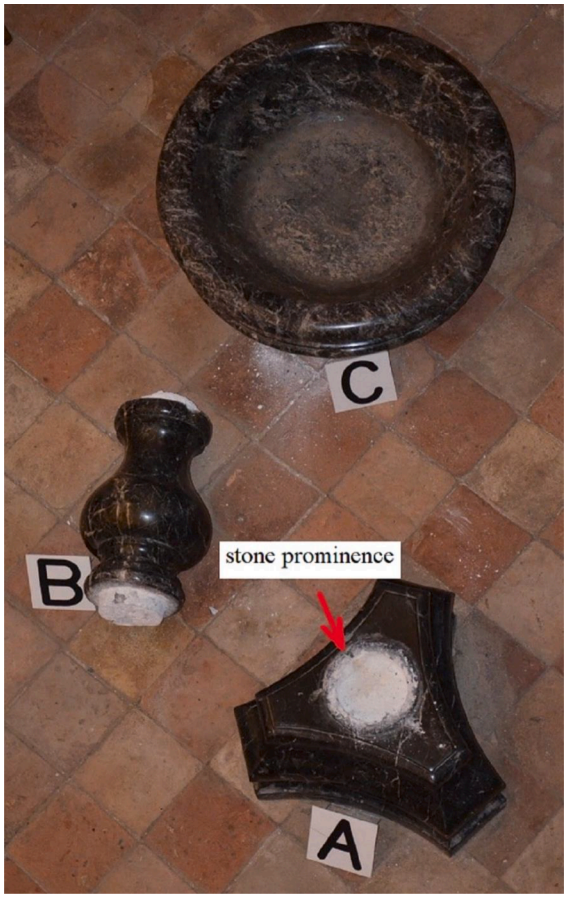

Fig. 3. Location of the holy water stoup elements on the floor of Santa Chiara Church after the accident.

Fig. 4. Stone prominence of the basement mortise.

is a diametrical play of 152 – 148 = 4 mm.

Comparing the tenon height and the mortise depth, it is derived that, between the ring around the mortise on the top of the basement and the ring around the tenon at the bottom of the shaft (Fig. 3), there is a vertical gap equal to 35.9 – 33.4 = 2.5 mm.

Moreover, on the basis of Fig. 5, it can be observed that there is also a play between the tenon and the prominence of the mortise equal to about 8 mm.

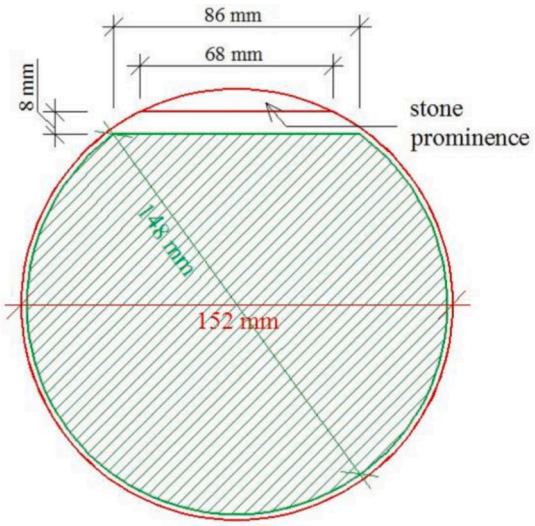

Fig. 5. Section of the basement-shaft connection in the plane containing the contact surface between the tenon and the mortise.

3.2. Basin-shaft connection

In the top connection, between the basin and the shaft, the tenon is at the top of the shaft and the mortise is at the bottom of the basin. The connection is conceived similarly to that between the basement and the shaft.

With regard to the tenon, the mean values of the diameter and height are equal to 155.7 mm and 39 mm, respectively.

The mortise is defined by a cylindrical hollow, of diameter 162 mm and depth 33.1 mm, having a circular segment plan-form stone prominence protruding from the top plane surface of the hollow.

From the comparison between the tenon and mortise diameters, a diametrical play of $162 - 155.7 = 6.3$ mm between the tenon and the basin mortise is derived.

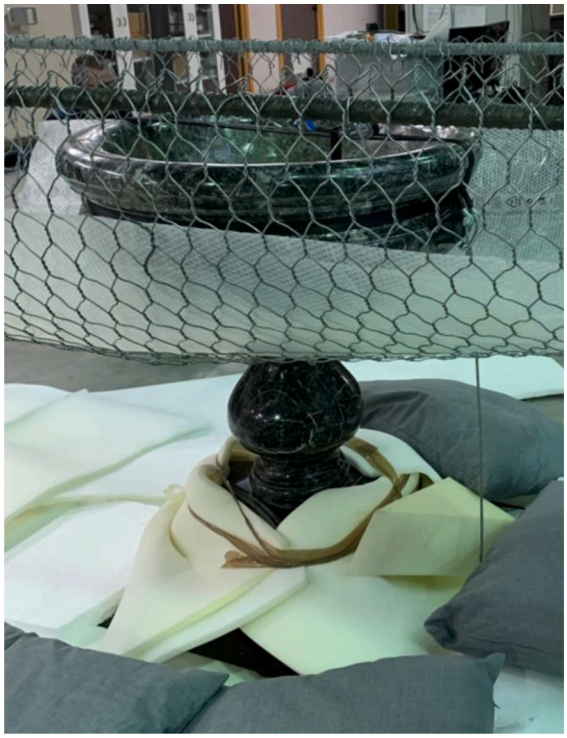

Fig. 6. Force application on the holy water stoup during the loading test.

Comparing the tenon height and the mortise depth, it can be found that, between the ring around the tenon at the top of the shaft and the ring around the mortise at the bottom of the basin, there is a vertical gap equal to 39 – 33.1 = 5.9 mm.

4. Laboratory tests and discussion of test results

In order to accurately model the kinematic behavior of the holy water stoup, some experimental tests are carried out. In particular, to evaluate the ability of the mortar to hinder relative displacements between the basement and the shaft and between the shaft and the basin, the mineralogical and petrographic analyses of a mortar sample taken from the holy water stoup are performed.

Moreover, to determine the failure load of the holy water stoup under a vertical force applied on the outer circumference of the basin, a loading test on the holy water stoup reassembled in the configuration before the collapse is carried out.

4.1. Mineralogical and petrographic analyses of the mortar

The analyses performed by the Laboratory of Ancient Materials Analysis of the University IUAV of Venice on the mortar sample show that the mortar is highly porous and it has a low aggregate amount. Moreover, it is found that the aerial lime constituting the mortar was not adequately cured and, thus, it results of poor quality. The mortar results particularly friable to the touch.

The results of the mineralogical and petrographic analyses of the mortar sample show that the mortar has a very low strength. Its strength is so low that it was unable to hinder relative displacements and rotations between the basement and the shaft and between the shaft and the basin, even under low forces. This leads to a not monolithic behavior of the holy water stoup. This conclusion, based on experimental results, is relevant since it identifies in the mortar ancientness a weak point of failure for all historical holy water stoups which have never been subjected to restoration interventions.

4.2. Loading test

The loading test is performed by the Mechanics of Materials Laboratory of the University IUAV of Venice. During the test a downward vertical force F is applied on the outer circumference of the basin, as it can be seen in Fig. 6 and represented in Fig. 7.

After the holy water stoup collapse on 21st November 2019, the shaft and the basin were found lying on the floor area opposite to the basement curved side adjacent to the stone prominence of the mortise, as it can be seen in Fig. 3. Also the kid was found, by the rescuers, in that floor area. It can be derived that the overturning of the shaft and the basin was caused by a tensile force applied by the kid on the basin side facing the stone prominence. For this reason during the loading test the force is applied at a point of the basin outer circumference above the stone prominence of the basement mortise.

The test is aimed at determining the value of the vertical force F involving the overturning of the holy water stoup. During the test the force F is gradually increased and the basin rotation around point O (Fig. 7) lying on the contact surface between the basin and the

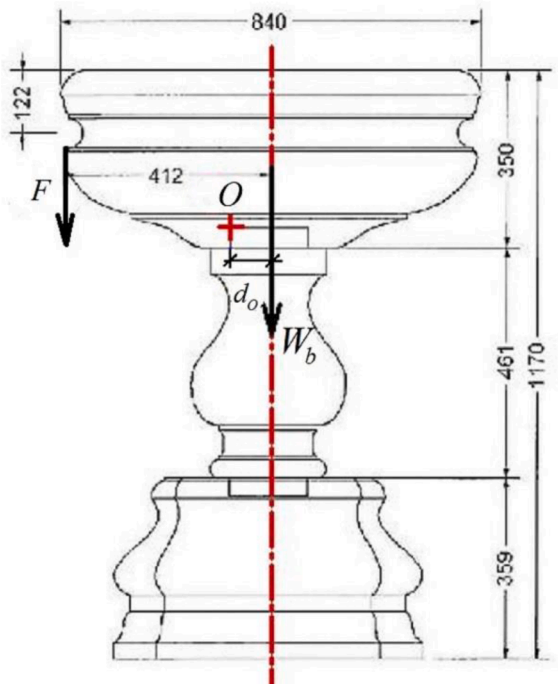

Fig. 7. Forces involved in the basin rotational equilibrium during the loading test (dimensions in mm).

shaft is observed, as shown in Fig. 8. The value of F that caused the basin overturning is equal to 513.9 N. At the end of the test, while the basin (block B1 in Fig. 1) has fallen, the shaft (block B2 in Fig. 1) is standing on the basement, in its original position.

The distance d_O of the rotation point O of the basin from the holy water stoup centroid axis, indicated with red dash-dot line in Fig. 7, can be obtained by solving the rotational equilibrium equation of the basin under the failure load obtained from the test, which can be derived from Eq. (1).

The forces involved in the overturning stability of the basin are the applied load F and the basin self weight W_b. Thus, for the considered case-study, Eq. (1) provides.

$$W_b \bullet d_O = F \bullet (d_F - d_O) \tag{4}$$

where d_F is the distance of force F application point from the basin centroid axis. This distance is equal to 412 mm, as shown in Fig. 7. Introducing the values of F and W_b, equal to 513.9 N and 1313.1 N, respectively, and the value of d_F in Eq. (4), it is obtained that $d_O = 74.3$ mm.

Since the mean value of the shaft top tenon diameter is equal to 155.7 mm, the radius mean value of the top tenon is equal to 78 mm. Being d_O smaller than the tenon radius, it follows that the rotation point O belongs to the top surface of the shaft top tenon. This is possible because the top surface of the shaft top tenon is not flat, but it is blunt along the edges. Thus, the perimeter line points of the rounded top surface of the shaft top tenon are at a lower altitude than the inner points of the surface.

5. Overturning stability analysis of the case study

The equilibrium analysis is made considering those configurations of the applied external force which are consistent with the observed collapse mechanism.

The equilibrium analysis of the holy water stoup is based on an accurate geometric and dimensional survey of the connections between the three rigid elements and on the results obtained from a static loading test carried out on the stoup in laboratory.

From the loading test it is obtained that the application of a downward vertical force tangent to the outer circumference of the basin involves the overturning of only the basin. Conversely, the collapse mechanism occurred on 21st November 2019 consists in the overturning of the shaft and the basin, as shown in Fig. 3. To have this type of mechanism, necessarily the initial act of motion that triggered the collapse has to be a rigid body rotation of the assembly composed by the basin and the shaft around a point B at the base of the shaft bottom tenon, actually unknown. In the initial act of motion the basin and the shaft rotate as a monolithic assembly, remaining integral each other. From the above it follows that, to involve the overturning of the shaft and the basin, a downward inclined force T applied at the top of the basin (point A in Fig. 9) has to be considered.

In particular, the horizontal component of T has to be high enough to cause the overturning of both the shaft and the basin, and not only of the basin around point O.

The aim of the analysis of the holy water stoup overturning stability presented in the following is to determine the values of T, statically applied at the top of the basin, involving the overturning of the shaft and the basin, for several values of the inclination angle,

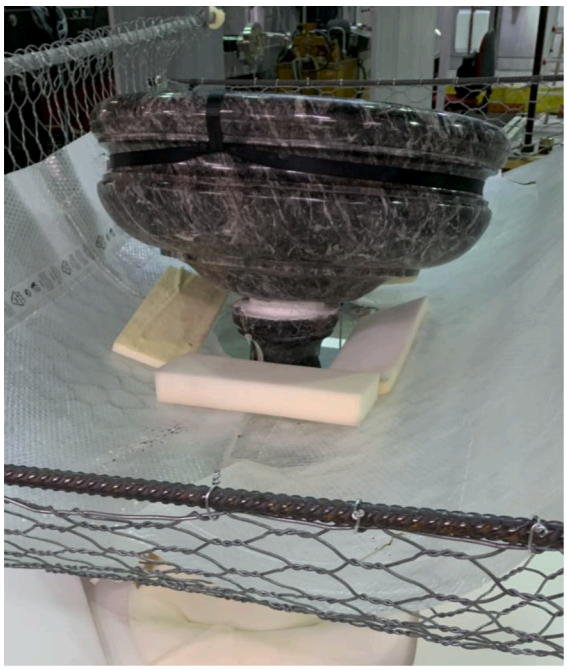

Fig. 8. Basin overturning observed during the loading test.

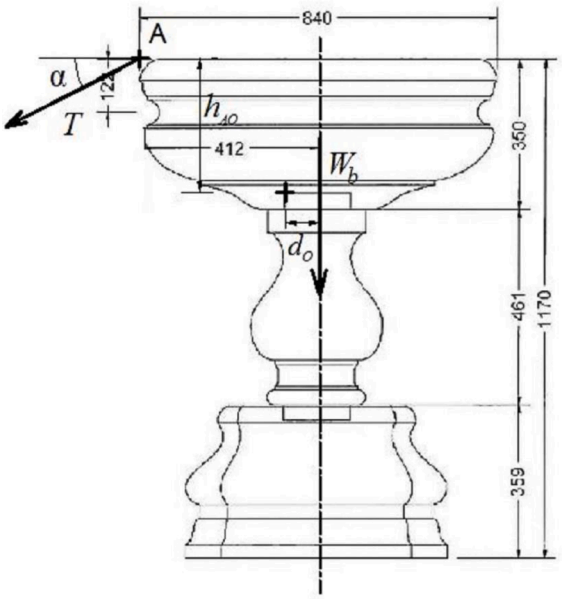

Fig. 9. Static scheme considered in the basin overturning collapse mechanism.

α, of T from the horizontal plane.

The range of α values involving the rotation of both the shaft and the basin is unknown. Thus, the values of T are determined in the α range from 0° (horizontal force) to 90° (vertical force), considering angles multiples of 5°. As said above, for $\alpha = 90°$, it is observed that the overturning of the only basin takes place. Thus, in the determination of T, both the collapse mechanisms 1 and 2, i.e. the overturning of the shaft and the basin as well as the overturning of the basin alone, have to be considered. Moreover, it is checked that mechanism 3, involving the whole assembly overturning, is characterized by ultimate loads higher than those involving mechanism 1 or 2.

Since the connections are not axisymmetric with respect to the holy water stoup centroid axis, the failure load values depend on the location of force T application point at the top of the basin (point A). In order to compute the force that the kid had to apply to the basin to involve the holy water stoup disarticulation really occurred, point A is assumed to be located in the vertical plane orthogonal to the

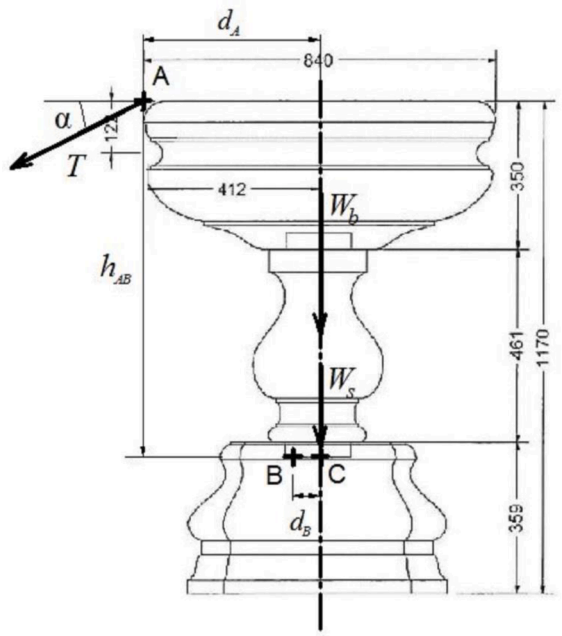

Fig. 10. Static scheme considered in the shaft-basin assembly overturning collapse mechanism (dimensions in mm).

rotation axis of the shaft and the basin during the collapse (Fig. 10), over the stone prominence in the basement mortise. For brevity, this plane is, in the following, named shaft and basin overturning plane.

On the basis of the mineralogical and petrographic analyses results, it is assumed that connections' geometrical plays evidenced in Sections 3.1 and 3.2 can be recovered without stress onset. Consequently, as regards the kinematic of the rigid blocks, it is considered that rotations, horizontal and upward vertical displacements of the basin relative to the shaft and of the shaft relative to the basement are allowed.

5.1. Mechanism 1: Basin overturning

Basin overturning collapse mechanism is that observed during the loading test previously described with reference to Fig. 7, and consists in the basin rotation around point *O*. Since the inclined force *T* is applied to the basin (Fig. 10), it has to be checked, for each α value considered in the analysis of the holy water stoup overturning stability, if it involves the basin overturning than the shaft-basin assembly overturning.

The forces involved in the rotational equilibrium of the basin are *T* and W_b, as shown in Fig. 9. Writing Eq. (1) for the considered case study, the rotational equilibrium of the basin around point *O* is expressed as follows.

$$W_b \bullet d_O = T\cos\alpha \bullet h_{AO} + T\mathrm{sen}\alpha \bullet (d_A - d_O) \tag{5}$$

5.2. Mechanism 2: shaft-basin assembly overturning

The rigid body rotation of the shaft-basin assembly occurs around a point *B* belonging to the boundary of the contact surface between the shaft bottom tenon and the basement mortise (Fig. 10). Assuming that the centroid vertical axes of the shaft and the basement are aligned, the contact surface coincides with the green hatched area in Fig. 5.

By the visual inspection of the holy water stoup elements at the site of the accident (see Fig. 3), two scratches on the upper surface of the basement, near the stone prominence of the mortise, are detected (Fig. 11). In particular, referring to Fig. 11, the scratch circled in green is caused by the friction between the shaft and the basement on the compression side, and the scratch outlined with a yellow rectangle is due to the collision of the shaft with the basement, during the collapse.

Moreover, still on the upper surface of the basement, at the opposite side of the stone prominence, damages on the hollow surface and on the ring around the hollow are detected. In particular, as it can be seen within the red outline in Fig. 11, marble split-up is observed. The damage is caused by the push action of the shaft bottom tenon against the lateral surface of the basement hollow, during the shaft rotation throughout the collapse mechanism.

In parallel, in the lower part of the shaft, at the location overlapping with that of the basement scratch outlined with a yellow rectangle in Fig. 11, a scratch is observed, which is outlined with a yellow rectangle in Fig. 12. Moreover, in the bottom tenon of the shaft, at the location overlapping with that of marble split-up in the basement, circled in red in Fig. 11, a chipping is ascertained, which is circled in red in Fig. 12.

In Fig. 12, joining the centroid of the chipping (point *E* in Fig. 12) and the scratch centroid (point *D* in Fig. 12) with a segment (red in Fig. 12) on the bottom surface of the shaft bottom tenon, it is observed that the segment passes through the centre *C* of the circle circumscribed around the tenon.

The drawn segment, *DE*, locates, on the contact surface between the shaft tenon and the basement mortise, the trace of the shaft and basin overturning plane.

As referred above, point *B* belongs to the boundary of the contact surface between the shaft tenon and the basement mortise. Given that the shaft and the basement were found lying on the floor area facing the stone prominence of the basement mortise, it is derived

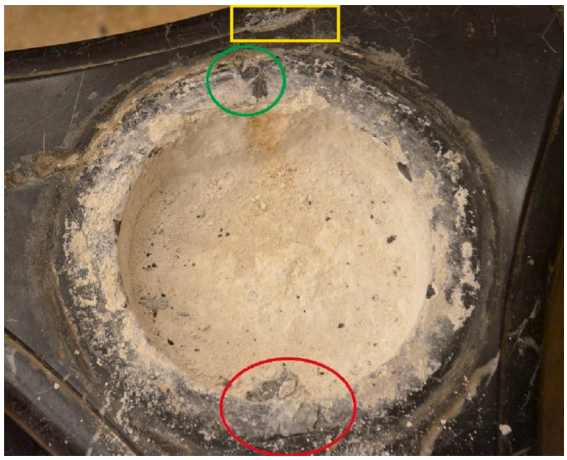

Fig. 11. Scratches and marble split-up at the upper surface of the basement.

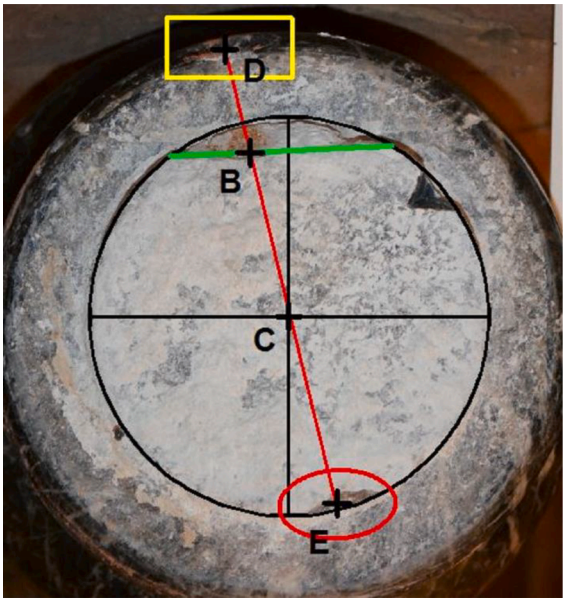

Fig. 12. Trace identification of the shaft and basin overturning plane on the lower surface of the shaft bottom tenon.

that point *B* lies on the straight side of the tenon indentation. Since point *B* belongs to the shaft-basin assembly overturning plane, it follows that point *B* is located at the intersection of the overturning plane with the straight side of the tenon indentation, as shown in Fig. 12. The distance between points *B* and *C*, d_{BC}, is found to be equal to 64 mm.

The rotational equilibrium of the shaft-basin assembly is governed by the applied force *T* and the self weights of the basin and the shaft, W_b and W_s, respectively (Fig. 10). Writing Eq. (2) for the considered case study, the rotational equilibrium of the assembly with respect to point *B* (Fig. 10) is expressed by the following equation.

$$(W_b + W_s) \bullet d_{BC} = T cos\alpha \bullet h_{AB} + T sen\alpha \bullet (d_A - d_{BC}) \tag{6}$$

5.3. *Mechanism 3: Whole assembly overturning*

The rotational equilibrium of the whole assembly is governed by the applied force *T* and the self weights of the basin, the shaft and the basement, W_b, W_s and W_f, respectively. Writing Eq. (3) for the considered case study, the rotational equilibrium of the assembly with respect to point *K* is expressed by the following equation.

$$(W_b + W_s + W_f) \bullet d_K = T cos\alpha \bullet h_{AK} + T sen\alpha \bullet (d_A - d_K) \tag{7}$$

6. Results

The values of force *T* involving the holy water stoup instability are calculated for each of the three collapse mechanisms described above.

Table 1
Values of force T obtained considering the basin collapse mechanism, for α values between 0° and 90°.

α (°)	T (N)	α (°)	T (N)
0	558.2	50	378.4
5	511.7	55	381.3
10	475.7	60	387.3
15	447.6	65	396.6
20	425.6	70	409.4
25	408.8	75	426.6
30	396.0	80	448.7
35	387.0	85	477.2
40	381.1	90	513.6
45	378.3		

6.1. Ultimate load for mechanism 1

Being the height mean value of the shaft top tenon equal to 39 mm, as reported in Section 3.2, from Fig. 9 it is derived that $h_{AO} =$ 311 mm.

Eq. (5) is solved for α values multiples of 5°, in the range from 0° to 90°. The values obtained for T are reported in Table 1.

6.2. Ultimate load for mechanism 2

Being the mean value of the shaft bottom tenon height equal to 35.9 mm, from Fig. 10 it is derived that $h_{AB} = 847$ mm. Still from this figure, it can be seen that $d_A = 412$ mm.

Eq. (6) is solved for the same α values considered in the resolution of Eq. (5) and the values obtained for T are reported in Table 2.

6.3. Ultimate load for mechanism 3

From the geometrical dimensions of the basement shown in Fig. 2(b) it is derived that, in the overturning plane observed in situ, the distance between point K and the assembly vertical axis, d_K, is equal to 234 mm. From Fig. 2(a) it can be seen that $h_{AK} = 1170$ mm.

Eq. (7) is solved for the same α values considered in the resolution of Eq. (5) and Eq. (6), and the values obtained for T are reported in Table 3.

6.4. Failure loads

For each of the considered α values, the failure load is given by the lowest of T values obtained from the three overturning collapse mechanisms, and reported in Table 1, Table 2 and Table 3. Comparing these tables it can be observed that the values of force T involving mechanism 3 (whole assembly overturning) are much higher than those involving mechanism 2 (shaft-basin assembly overturning) and mechanism 1 (overturning of the basin alone). In particular, the ratio between the ultimate load of mechanism 3 and the higher ultimate load of mechanisms 1 and 2, for $\alpha = 0°$, is equal to 832.4 N/558.2 N = 1.49, and for $\alpha = 90°$, is equal to 5236.0 N/524.1 N = 9.99. For this reason, for the determination of the failure loads, only the ultimate loads involving the basin overturning, reported in Table 1, and those involving the shaft-basin assembly overturning, reported in Table 2, are considered in the following.

In Fig. 13, the T values from these tables are diagrammed versus α. From Fig. 13 it is observed that, for $0° \leq \alpha \leq 85°$, the values of force T involving the overturning of the shaft-basin assembly are lower than those involving the overturning of the basin alone. It can be concluded that the application of a force T at point A at the top of the basin, belonging to the shaft and basin overturning plane observed in situ, involves the overturning of the shaft-basin assembly whatever the inclination angle, α, is, for α values between 0° and 85°.

Moreover, it can be observed that, by considering α values between 0° and 90° with an increment of 5°, only for $\alpha = 90°$ the collapse mechanism involved by force T coincides with the basin overturning. In this case the failure load coincides with that derived experimentally from the loading test.

Still from Fig. 13, it can be observed that the minimum force value for the shaft-basin assembly overturning mechanism, equal to 198.7 N, is attained for $\alpha = 20°$. This is the most dangerous inclination at which one can apply the force T, in the considered case.

It is noteworthy that, in relation to the geometric and weight properties of the holy water stoup, the collapse mechanism and the most dangerous inclination of the applied force can change.

7. Discussion of results

From the analysis of the case study it is obtained that the collapse is caused by mechanism 2. The occurrence of mechanism 2, instead of mechanisms 1 and 3, is confirmed by the fact that, after the accident, both the shaft and the basin were found lying on the floor, while the basement was in its original position. In particular, the shaft and the basin were lying in front of the basement curved side facing the stone prominence in the basement mortise, as referred in Section 5.2. This position of the elements is compatible with that caused by mechanism 2.

In order to check the suitability of the performed analysis in the evaluation of the failure loads for the considered case-study, it has to be assessed if the obtained load values could be applied by the kid who produced the stoup overturning, in relation to her build. With this aim, the values of force T reported in Table 2 are compared with the kid's weight, equal to 265 N. Actually, when someone hangs on a support with his arms vertically arranged, the force sustained by the arms is equal to the person's weight. Accordingly, it can be stated that a person, even a kid, is able to bear and, hence, apply, a traction force equal to his/her weight. From the comparison with the kid's weight, it is observed that the failure loads obtained for $0° \leq \alpha \leq 60°$ are lower than 265 N. Thus, it can be concluded that the performed stability analysis is able to confirm that the disarticulation of the holy water stoup could be caused by a force applied by the kid at the top of the basin, under static load conditions. This discovery is very important, because low forces, as the one applied by the kid, can be applied also by elderly or disabled people who can lean against the basin to have a support, or even by adults who, during Mass, can lean against the basin.

Moreover, comparing the lowest ultimate load involving mechanism 3, equal to 832.4 N (Table 3), with the kid weight, it can be derived that the kid alone was not able to involve the holy water stoup overturning (mechanism 3). From this result it can be drawn that providing a monolithic behavior to the assembly, by stabilizing the connections between the rigid blocks, is of the greatest

Table 2
Values of force T obtained considering the shaft-basin assembly collapse mechanism, for α values between 0° and 90°.

α (°)	T (N)	α (°)	T (N)
0	215.3	50	224.9
5	208.7	55	236.6
10	203.9	60	251.6
15	200.8	65	270.9
20	199.4	70	295.8
25	199.4	75	328.4
30	201.0	80	372.4
35	204.2	85	433.8
40	209.0	90	524.1
45	215.9		

Table 3
Values of force T obtained considering the whole assembly collapse mechanism, for α values between 0° and 90°.

α (°)	T (N)	α (°)	T (N)
0	832.4	50	1088.7
5	824.1	55	1182.7
10	822.2	60	1305.4
15	826.5	65	1468.8
20	837.4	70	1693.9
25	855.1	75	2018.5
30	880.4	80	2520.8
35	914.4	85	3390.3
40	958.7	90	5236.0
45	1015.7		

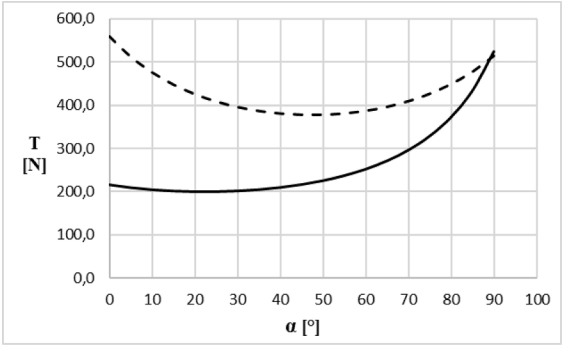

Fig. 13. Force T values versus α, for the basin (dashed line) and the shaft-basin assembly (continuous line) overturning collapse mechanisms.

importance in order to avoid assembly disarticulation. In fact, connection stabilization makes possible only the occurrence of mechanism 3 that requires very high forces, at least of 832.4 N, which are not compatible with a single person action and, in particular, with accidental actions exerted even by an adult.

8. Preventive actions against stoups failure

To determine if preventive actions against stoups overturning mechanisms need to be adopted, the ultimate loads obtained from each mechanism has to be compared with adequately safe limit values. In particular, for $\alpha = 0°$ (i.e. horizontal load), the values of T can be compared with that prescribed by UNI EN 13374:2019 [13] for temporary edge protection systems at the ultimate limit state. This value is equal to 450 N.

For $\alpha = 90°$ (i.e. vertical load), the upper bound can be taken equal to the weight of a human being with stocky build, which can be assumed equal to 900 N. This condition is the one that occurs when a person with this build hangs on the basin with his arms vertically arranged.

For $0° < \alpha < 90°$, the horizontal and the vertical components of the ultimate loads T obtained from mechanisms 1, 2 and 3 must be

lower than 450 N and 900 N, respectively.

By comparing the values of T for $\alpha = 0^\circ$ and $\alpha = 90^\circ$ obtained from mechanisms 1 with the respective limit bounds, it can be assessed if the connection between the basin and the shaft need to be stabilized. Analogously, when the values of T obtained from mechanisms 2 for $\alpha = 0^\circ$ and $\alpha = 90^\circ$ are lower than the respective limit bounds mentioned above, the connection between the basement and the shaft need to be stabilized. Similarly, if the values of T obtained from mechanism 3 for $\alpha = 0^\circ$ and $\alpha = 90^\circ$ are lower than the respective upper bounds, in order to avoid mechanism 3, it is necessary to anchor the basement to the ground.

The stability of stoups with pillar realized as three rigid block assemblies, with tenon and mortise connections, can be obtained by casting anti-shrinkage mortar in the mortise, filling the whole space between the mortise and the tenon. Otherwise the stability of connections can be provided by stainless steel threaded bars or studs placed in the holes realized in the three elements. In particular, with regard to the basement-shaft connection, a stud with diameter of about 3 cm can be embedded in each element and the bond between the stone elements and the stud can be guaranteed by epoxy resin or mortar. While, with regard to the shaft-basin connection, a pre-tensioned threaded bar can be anchored into the shaft and placed into the through hole realized in the basin.

In alternative, a single threaded bar anchored into the basement can be passed through the holes realized in the shaft and the basin. The bar is then pre-tensioned and the nut emerging from the basin is covered by a cap or mortar layer.

Finally, to avoid the overturning of the whole assembly, the anchoring of the basement to the floor can be obtained by casting anti-shrinkage mortar between the basement and the floor, or by a threaded bar, anchored into the floor, passing through the hole realized in the basement.

9. Conclusions

The present study highlights, for the first time, the importance of the structural problem of stability of rigid block assemblies, as well as the various factors influencing their overturning.

On the basis of the above, the following conclusions are drawn:

1) Overturning stability of three rigid block assemblies, as are some historical assets, can be analyzed considering the three possible collapse mechanisms.

2) Historical artistic assets, as holy water stoups, may be characterized by high structural vulnerability. The great number of accidents due to disarticulation of holy water stoups realized as rigid block assemblies highlights that the collapse risk of these historical structures is high. For this reason, holy water stoups has to be treated as any other permanent and/or temporary structure open to the public, with the safety requirements imposed by the related legal obligations, in particular the adequate safety against failure and overturning.

It is derived that the overturning stability of these stoups has to be adequately assessed by those responsible for the safety assessment of churches or other places where they are located, in order to adopt adequate safety measures.

3) The case study discussed in this research highlights the importance to assess the safety of architectural and historical objects respect to all possible collapse mechanisms which can be dangerous for human life, to guarantee that visitors could enjoy the cultural heritage in safe conditions.

The holy water stoup considered in the case study was not protected against external forces by barriers or other safety measures that could avoid the contact with people.

4) In the case of objects realized as rigid block assemblies, it is fundamental to ascertain that linking materials are able to stabilize the connections between the rigid blocks and provide a monolithic behavior to the assembly. Consequently, the age of construction plays an important role. In particular, mortar ancientness represents a weak point of all holy water stoups that have never been subjected to restoration interventions.

5) In order to properly model the kinematic behavior of rigid block assemblies, an accurate geometrical and dimensional survey of connections is fundamental. For the considered case-study, the geometrical and dimensional survey of tenons and mortises shows the presence of vertical gaps and diametrical plays in the basement-shaft and shaft-basin connections. As a consequence, rotations, horizontal and upward vertical displacements of the basin relative to the shaft and the shaft relative to the basement can occur.

6) If tenons and mortises are not axisymmetric with respect to the holy water stoup centroid axis, the position of the rotation point in the basin and in the shaft-basin assembly overturning collapse mechanisms depends on the location of the external force application and force direction.

7) A general analytical method for the overturning stability analysis of three rigid block assemblies, composed by three blocks fitted atop one on another, is proposed. The method allows to calculate the ultimate loads of assemblies with respect to all possible overturning collapse mechanisms, for different load configurations, described by the inclination angle of the load, α, from the horizontal plane. For each of the considered α values, the failure load coincides with the lowest ultimate load obtained from all the collapse mechanisms 1, 2 and 3. This load is the lowest value of the three curves representing the ultimate load in function of α for each collapse mechanism.

8) The method used for the overturning stability analysis of the considered case-study is general, since, considering both the basin and the shaft-basin assembly overturning collapse mechanisms, varying the angle of inclination α, it provides the lowest force able to involve the holy water stoup disarticulation. Thus, the proposed method represents a simple and practical tool for the overturning stability assessment of holy water stoups with pillar under static load conditions.

9) Regarding the collapse mechanism of the stoup under study, the shaft-basin assembly overturning in the considered case-study occurs for the range of force inclination α between 0° and 85°. Otherwise, for inclination of 90° the basin overturning occurs. For a stoup with different geometry and weight of the three blocks the α range in which the basement-shaft assembly overturning occurs can

 result different.

It follows that, to assess the overturning stability of the rigid block assemblies, the failure load has to be determined in the most unfavourable load configuration.

10) Some proposals of preventive actions against failure are shown.

Declaration of Competing Interest

The authors declare that they have no known competing financial interests or personal relationships that could have appeared to influence the work reported in this paper.

Data availability

No data was used for the research described in the article.

Acknowledgements

Authors wish to acknowledge the engineer Franco Curtarello, Public Prosecutor's expert in the manslaughter proceeding occurred in the considered case study, for the effort in supporting the need of performing experimental tests on the stoup.

The research has been partially funded by the Italian Department of Civil Protection (within the framework of Executive Project DPCReLUIS 2019–2021), whose support is greatly appreciated.

The research has been partially funded also by the strategic plan of University of Udine within the framework of the project "ESPeRT".

References

[1] Bambina morta schiacciata dall'acquasantiera: inchiesta per omicidio colposo. Il gazzettino, edition of 22nd November 2019. Available online: https://www.ilgazzettino.it/nordest/udine/bambina_morta_schiacciata_acquasantiera_inchiesta_ultime_notizie-4879705.html (accessed on 25 May 2022).
[2] Schiacciata da un'acquasantiera durante l'ora di religione: muore bambina. TGR Friuli Venezia Giulia, edition of 21st November 2019. Available online: https://www.rainews.it/tgr/fvg/articoli/2019/11/fvg-bimba-morta-travolta-acquasantiera-udine-b6b8b4b4-f707-4f91-b7d1-39feb76989fe.html (accessed on 25 May 2022).
[3] Udine, bambina di 7 anni muore in chiesa: l'acquasantiera le è caduta addosso. The Post Internazionale, edition of 22nd November 2019. Available online: https://www.tpi.it/cronaca/bambina-morta-acquasantiera-udine-20191122502582/ (accessed on 25 May 2022).
[4] Un bimbo muore schiacciato in chiesa dall'acquasantiera. L'Unità, edition of 14th April 1971. Available online: https://archivio.unita.news/assets/main/1971/04/14/page_009.pdf (accessed on 25 May 2022).
[5] La Nuova, edition of (10th August 1996.).
[6] Muore in chiesa bimbo di 4 anni. La Repubblica, edition of 11th April 2001. Available online: https://ricerca.repubblica.it/repubblica/archivio/repubblica/2001/04/11/muore-in-chiesa-bimbo-di-anni.html (accessed on 29 January 2022).
[7] Bimbo schiacciato da acquasantiera. SiciliaTv.org. Available online: https://siciliatv.org/2003/05/06/bimbo-schiacciato-da-acquasantiera/ (accessed on 29 January 2022).
[8] Bimbo di sei anni travolto dall'acquasantiera dentro la chiesa. Treviso today, edition of 28th March 2014. Available online: https://www.trevisotoday.it/cronaca/acquasantiera-caduta-incidente-chiesa-bambino-mareno-di-piave.html (accessed on 29 January 2022).
[9] Alfianello: crolla l'acquasantiera, bimbo di 11 anni in pericolo di vita. Brescia today, edition of 21th February 2015. Available online: https://www.ilgiorno.it/brescia/cronaca/ferito-chiesa-1.693779 (accessed on 29 January 2022).
[10] Cede l'acquasantiera e ferisce un bambino fratturandogli il piede. Gazzetta di Mantova, edition of 28th October 2018. Available online: https://gazzettadimantova.gelocal.it/mantova/cronaca/2018/10/28/news/cede-l-acquasantiera-e-ferisce-un-bambino-fratturandogli-il-piede-1.17400624 (accessed on 29 January 2022).
[11] A.N. Kounadis, G.J. Papadopoulos, On the rocking instability of a three-rigid block system under ground excitation, Arch. Appl. Mech. 86 (2016) 957–977.
[12] M. Kovács-Bende, Response of rigid block assemblies to earthquake excitation. Periodica Polytechnica, Mech. Eng. 44 (1) (2000).
[13] UNI EN 13374:2019. Temporary edge protection systems – product specification – Test methods.